Catalytic bromination of anthracene on silica gel

Jorma A. Seetula *

Laboratory of Physical Chemistry, P.O. Box 55, A.I. Virtasen aukio 1, University of Helsinki, FIN 00014 Helsinki, Finland

Abstract

The heterogeneous kinetics of the catalytic bromination of anthracene ($C_{14}H_{10}$) on silica gel has been investigated in situ as a function of temperature in a static mode using a dual beam absorptiospectrophotometer and a spectrofluorophotometer. The surface of the silica gel was treated by Br_2 diluted to CCl_4 solvent. Adsorption rate of the reactants or the products of the reaction on pure silica gel surfaces, and a liquid phase bromination reaction of the reactants were very slow compared to the overall kinetics measured. The reactions were studied under first-order conditions. Anthracene was brominated catalytically fast to produce 9-bromoanthracene as the only aromatic product of the reaction. Arrhenius activation energy of the 9-bromoanthracene formation was determined to be $50.33 \pm 0.23\,kJ\,mol^{-1}$ at temperature range from 294 to 345 K. Furthermore, 9-bromoanthracene was brominated catalytically relatively fast to produce 9,10-dibromoanthracene, which was not possible brominate any further at the experimental conditions used. The rate of the 9-bromoanthracene formation was by a factor of 4.2 ± 2.8 higher than that of the 9,10-dibromoanthracene formation. The kinetics of the substitution reactions were investigated by measuring the increase of the 9-bromoanthracene absorption signal at 392 nm or the 9,10-dibromoanthracene absorption signal at 405 nm, or the decrease of the anthracene fluorescence signal at 386 nm or the 9-bromoanthracene fluorescence signal at 397 nm. The heat of the overall bromination reaction of the anthracene to yield the 9-bromoanthracene was measured calorimetrically to be $-59.1 \pm 2.4\,kJ\,mol^{-1}$ at $293.6 \pm 0.8\,K$.
© 2004 Elsevier B.V. All rights reserved.

Keywords: Kinetics of bromination; SiO_2; Anthracene; 9-Bromoanthracene; 9,10-Dibromoanthracene

1. Introduction

One of a well known straight forward syntheses, which does not require any special laboratory technique, is bromination of anthracene [1–4]. Nowadays, typically, 9-bromoanthracene is prepared from it by a brominating agent or by adding bromine to a solution of anthracene in ethyl acetate. The reaction is catalysed by anhydrous iron(III) chloride and by heating the reaction mixture gently. The addition product of the reaction formed is later dehydrohalogenated by refluxing the solution over several hours [5]. Quite recently, Ghiaci and Asghari studied a series of silica gel catalysed bromination reactions of aromatic compounds at room temperature and observed the reaction of anthracene with bromine to be relative fast and to produce only 9,10-dibromoanthracene and HBr with high yield [6]. They did not investigate the kinetics or the dynamics of

the reaction at all. The kinetics of anthracene bromination reaction has been studied in some extent by Altshuler and Berliner, but at different experimental conditions as those used in the current study [2].

This study represents an experimental kinetic, thermodynamic and spectroscopic investigations of anthracene molecules with bromine in a non-polar liquid. The bromination reaction is catalysed by hydrated silicon–oxygen, i.e. silica gel. The kinetics of the catalyzed reaction has not previously been studied. The dynamics of the reaction is re-investigated here in order to examine intramolecular electronic effects which affect the extend of the bromination.

2. Experimental

2.1. Description of experiments

Kinetic experiments were measured in situ by means of spectroscopic methods. Two different techniques were used.

* Tel.: +358 919150284; fax: +358 919150279.
  E-mail address: seetula@csc.fi.

Table 1
Recorded absorption and fluorescence signal maximums in nm of anthracene, 9-bromoanthracene, and 9,10-dibromoanthracene in CCl_4

Molecule	Absorption signals	Fluorescence signals
$C_{14}H_{10}$	265, 311.5, 326.2, 342.2, 359.5, 378.8	386.8, 406.8, 429.2, 455, 490
9-$C_{14}H_9Br$	266, 321.3, 336.3, 353.2, 371.7, 392.3	397.2, 421.6, 444, 471
9,10-$C_{14}H_8Br_2$	267, 313.3, 328.3, 345.7, 363.2, 383.2, 405.2	412.8, 437.2, 461.2, 490

Firstly, the absorption spectra were recorded by use of a dual beam Cary 100 spectrofotometer with a resolution of 0.5 nm. The quartz absorption cells of 10 mm light path length used with a thermostattable cell holder were coupled to a thermostatting bath to maintain a constant temperature of 294.0 ± 0.5 K in the cells. The sample cell contained typically 2.0 ml 0.0004 M anthracene in CCl_4 or 2.0 ml 0.0004 M 9-bromoanthracene, completely brominated silica gel in varying amounts and a special kind of cuvette stir bar, which provided efficient horizontal and vertical mixing by means of a magnetic stirring of the reactants with a minimum vortex formation or aeration. For further bromination reactions typically 1.0 ml 0.004 M Br_2 in CCl_4 was added to the sample cell.

One set of experiments were also measured as a function of temperature. The formation of the 9-bromoanthracene in absence of silica gel was measured at temperature range from 294 to 345 K, where the upper limit was determined by the boiling point of the solvent.

For kinetic experiments the 9-bromoanthracene absorption signal was recorded as a function of time at 392 nm and the 9,10-dibromoanthracene absorption signal at 405 nm, respectively. The recorded UV absorption spectra of the anthracene, [7] the 9-bromoanthracene and the 9,10-dibromoanthracene were also compared to the spectra of the pure compounds found in [7,8].

Second, the fluorescence spectra were recorded by use of Shimadzu RF-5000 spectrofotometer with a resolution of emission radiation of 1.5 nm. The fluorescence spectrum of the anthracene starts at 387 nm. For the 9-bromoanthracene it starts at 397 nm and for the 9,10-dibromoanthracene, at 413 nm. For producing last two compounds, the surface of the silica gel was brominated before the anthracene or the 9-bromoanthracene was added to the cuvette. There was no Br_2-containing CCl_4 present. The reactants were efficiently mixed during the kinetic experiment. Temperature in the cell during the reaction was 301 ± 1 K. For the kinetic experiments, the fluorescence decay signal of anthracene was obtained by exciting the anthracene at wavelength of 359.3 ± 1.5 nm. The emission radiation at 386 ± 1.5 nm was recorded at a right angle compared to the exciting radiation at the peak of the reactant fluorescence signal. In separate experiments, the kinetics of the 9-bromoanthracene decay was monitored at 397.2 ± 1.5 nm by exciting the 9-bromoanthracene at wavelength of 336.0 ± 1.5 nm (see Table 1).

The heat of the reaction was studied calorimetrically. These measurements were done by means of Parr 1455 Solution Calorimeter. Typically 100 ml of a concentrated

$C_{14}H_{10}$-containing (or 9-$C_{14}H_9Br$-containing) CCl_4 liquid was placed in a Dewar and varying amounts of Br_2 diluted in 5.0 ml of CCl_4 liquid was placed into a rotating cell, made of a Teflon Dish and class walls, of the calorimeter. After the reactants came to thermal equilibrium, the reaction was started and the temperature change was measured in situ by a thermistor. The thermogram was recorded for further analysis. The solvent of the solution was evaporated and the solid product was later dissolved into $CDCl_3$ and analyzed by measuring its ^1H NMR spectrum. The nuclear magnetic resonance measurements were done by means of Varian Inova 300 MHz NMR spectrophotometer.

2.2. Data analysis

A general rate law of a competitive adsorption of the various components of the system under first-order conditions on the saturated catalyst can be written as shown in Eq. (1) [9]:

$$v = k \left[\frac{b_R[R]}{1 + b_R[R] + b_P[P] + b_S[S]} \right] \quad (1)$$

Here R is a reactant, P and S are the products and b_i stands for the adsorption coefficient of the species. The equation is based on the Langmuir isotherm. In the case were all species have very small affinity for the catalyst, the Eq. (1) simplifies and $b_i[i]$ are very small and can be neglected in the denominator. Then the rate law appears to be first-order respect to the reactant: $v = kb_R[R] = k'[R]$, and the apparent rate coefficient is the product of the true rate constant and the adsorption coefficient. The rate coefficients in the current study were obtained from a first-order exponential decay of $[R]_t = [R]_0 \exp(-k't)$ of the reactant or a first-order exponential rise of $[P]_t = [P]_0\{1 - \exp(-k't)\}$ of the product. Magnitude of the k' depends on the surface area of the brominated catalyst. Moreover, no intermediates were detected during the reactions, no liquid phase bromination reaction was present, the solvent did not react with reactants or products, and did not poison the catalyst used.

The heat capacity of the empty Dewar of the calorimeter was determined by calibrating it with a known amount of the sample of tris(hydroxymethyl)aminomethane. The molar heat of the bromination reaction was calculated by means of Eq. (2):

$$\Delta_r H = -\frac{\Delta TE}{m} \quad (2)$$

Here ΔT is the temperature change of the reaction determined from the recorded thermogram, m the mass of the $C_{14}H_{10}$ (or 9-$C_{14}H_{10}Br$) and E includes the energy equivalent of the Dewar flask and the specific heat capacity of the solvent [10].

2.3. Accuracy of measurements

The error limits stated in kinetic expressions are 1σ + Student's t and based only on the statistical uncertainties. The conditions of the reactions were pseudo-first-order, where it was needed to known as accurately as possible the amount of brominated silica gel present. This was, however, difficult to measure more precisely than with accuracy of 2 mg. Moreover, the ratio of activated/deactivated silica gel surface sites may make this accuracy worse than expected. To minimize the amount of deactivated surface sites of the catalyst, the silica gel was kept at constant temperature of 373 K at least 24 h before using it in the experiments. The other errors during the reaction including the accuracies in concentrations of anthracene and bromine, and the accuracy of temperature, were small and thus ignored.

The walls of the Dewar catalyzed the bromination reactions in the calorimetric measurements. The reactants were weighted with accuracy of 2 mg and the solvent was measured volumetrically with accuracy of 0.5 ml. During the reaction the initial and the final temperatures of the reactions were recorded with accuracy of 0.00001 K, whereas a typical temperature change was about 0.43 K.
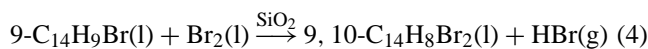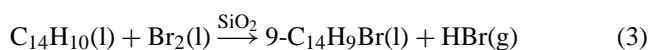
2.4. Reagent sources

Anthracene (99%), 9-bromoanthracene (94%), 9,10-dibromoanthracene (98%), and Br_2 (99.99%) were obtained from Aldrich, CCl_4 (99.9995%) was obtained from Riedel-deHaën, and silica gel 60 (230–400 mesh, Bet surface area 480–540 $m^2\,g^{-1}$ for column chromatography) was obtained from Merck. The silica gel was kept at 100 °C at least 24 h before using it, all other reagents were used as provided.

3. Results

3.1. Kinetic and calorimetric results

The chemical kinetics of the following heterogeneous catalytic reactions were studied separately:

$$C_{14}H_{10}(l) + Br_2(l) \xrightarrow{SiO_2} 9\text{-}C_{14}H_9Br(l) + HBr(g) \qquad (3)$$

$$9\text{-}C_{14}H_9Br(l) + Br_2(l) \xrightarrow{SiO_2} 9,10\text{-}C_{14}H_8Br_2(l) + HBr(g) \quad (4)$$

The results obtained from the experiments to measure reactions (3) and (4) are given in Table 2 and Fig. 1. The slopes of the plots in the figure are $(1.79 \pm 0.11) \times 10^{-3}\,mg^{-1}\,s^{-1}$ for the 9-bromoanthracene formation and $(0.40 \pm 0.03) \times 10^{-3}\,mg^{-1}\,s^{-1}$ for the 9,10-dibromoanthracene formation.

Before kinetic experiments both absorption and fluorescence spectra of the compounds were measured. Absorption

Table 2
Measurements of the rate coefficient k' of the catalytic bromination reactions

Silica gel (mg)	$k'(9\text{-}C_{14}H_9Br)^a$ ($\times 10^{-2}\,s^{-1}$)	$k'(9,10\text{-}C_{14}H_8Br_2)^a$ ($\times 10^{-2}\,s^{-1}$)	$k'(C_{14}H_{10})^b$ ($\times 10^{-2}\,s^{-1}$)	$k'(9\text{-}C_{14}H_9Br)^b$ ($\times 10^{-2}\,s^{-1}$)
0	<0.001	<0.0001		
7	1.70 ± 0.03	0.274 ± 0.005	1.108 ± 0.004	
7		0.158 ± 0.003		0.377 ± 0.002
10	1.51 ± 0.06	0.306 ± 0.011		
15	1.91 ± 0.01		1.817 ± 0.009	
16	1.85 ± 0.01			
17	2.35 ± 0.05	0.528 ± 0.006	1.593 ± 0.015	
18		0.450 ± 0.001		
18		0.455 ± 0.005		
20	2.39 ± 0.05	0.422 ± 0.007		
23		0.576 ± 0.006		0.702 ± 0.003
25	4.53 ± 0.07	0.693 ± 0.011		
26	4.65 ± 0.10		3.69 ± 0.02	
27				0.957 ± 0.005
31	4.40 ± 0.04	1.384 ± 0.007		
33	6.2 ± 0.2	0.971 ± 0.011		
38	6.41 ± 0.10	1.308 ± 0.006	5.26 ± 0.03	
41				1.277 ± 0.053
41				1.247 ± 0.006
43	7.8 ± 0.3	1.44 ± 0.02		
44		1.75 ± 0.02		
48	7.14 ± 0.10	1.75 ± 0.02		
55			9.91 ± 0.06	
57				2.331 ± 0.014

[a] A rise coefficient k', errors limits are standard errors from the curve-fitting algorithms.
[b] A decay coefficient k', errors limits are standard errors from the curve-fitting algorithms.
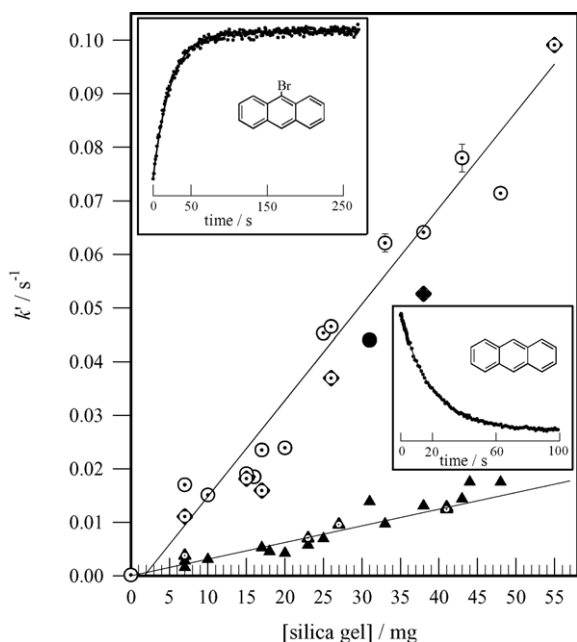
Fig. 1. Plots of first-order rise constant k' vs. $m_{silica\ gel}$ for the set of experiments to measure the catalytic bromination of anthracene (open circles) or 9-bromoanthracene (solid triangles) on the silica gel at 294 K from absorption measurements. The first-order decay constant values of anthracene or 9-bromoanthracene from fluorescence measurements are shown as open diamonds and open triangles. The inset in the upper left corner is the absorption signal profile of 9-$C_{14}H_9Br$ recorded during one of the experiments shown as a solid circle ($m_{silica\ gel} = 31$ mg) in the linear regression fit. The line through the data in the inset is an exponential function of the product fitted using the Marquardt–Levenberg algorithm. The inset in lower right corner is the fluorescence signal of $C_{14}H_{10}$ recorded during one of the experiments shown as a solid diamond ($m_{silica\ gel} = 38$ mg). The line through the data in the lower inset is an exponential decay function of the reactant fitted using the Marquardt–Levenberg algorithm.

spectra of the anthracene, the 9-bromoanthracene, and the 9,10-dibromoanthracene were recorded from 220 to 420 nm with a spectral resolution of 0.5 nm (Fig. 2). All the spectra measured had a very strong absorption at 266 ± 1 nm and a much weaker electron vibration band of 5 or 6 peaks existing from 311 to 405 nm. Fluorescence spectra were recorded between wavelengths of 380 and 600 nm with a spectral resolution of 1.5 nm, respectively. The fluorescence spectra had four emission bands. Spectral information is given in Table 1.

The kinetic data was collected as a function of time by means of spectroscopic methods. All of the absorbance signals in kinetic experiments were recorded at conditions where the concentrations of reactants were low enough to obey the Beer–Lambert law. A typical kinetic data point, as shown in Fig. 1 in the inset, is an average of absorbances regarded 0.5 s at the peak of the product absorbance signal. The delay between the data points collected was typically 1.0 s. In a similar manner the fluoresencense signals were recorded at 0.6 s time interval at the peak of the reactant fluorescence signal. Furthermore, the first-order rate laws of the decay or rise signals were fitted to the set of data points collected by the Marquardt–Levenberg algorithm to obtain the best fit
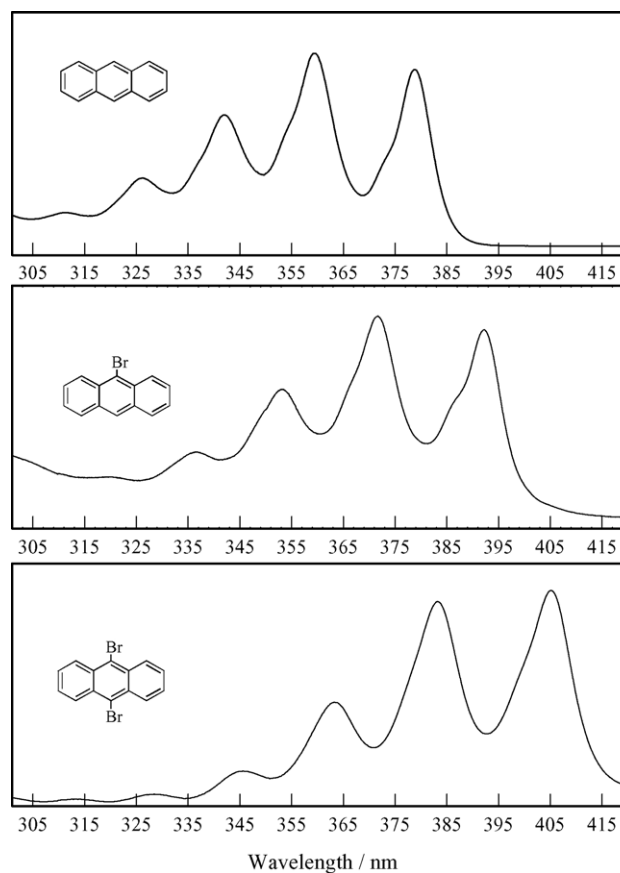

Fig. 2. UV absorption spectra of anthracene, 9-bromoanthracene, and 9,10-dibromoanthracene isolated in CCl_4. The resolutions of the spectra were 0.5 nm. Concentrations of the samples were 2×10^{-4} M.

between the rate equation and the data points. Correlation coefficients of these fittings were in the range from 0.98 to 0.99. The relative rates for reactions (3) and (4) were obtained from the slopes of the plots of the exponential rise (or decay) constant k' versus $m_{silica\ gel}$.

In the calorimetric measurements the heat of the overall catalytic bromination of the $C_{14}H_{10}(l)$ to yield the 9-$C_{14}H_9Br(l)$ was obtained to be -59.1 ± 2.4 kJ mol^{-1}. Table 3 gives the results and experimental conditions for the calorimetric experiments. For the 9-$C_{14}H_9Br$, the ^{1}H NMR: $\delta(CDCl_3)$ 8.54 (d, 2H), 8.45 (s, 1H, H_{10}), 8.01 (d, 2H), 7.64–7.49 (m, 4H), and for the 9,10-$C_{14}H_8Br_2$ the ^{1}H NMR: $\delta(CDCl_3)$ 7.66–7.62 (m, 4H), 8.61–8.58 (m, 4H).

3.2. Temperature dependency of the 9-bromoanthracene formation

Temperature dependency of the 9-bromoanthracene formation was investigated in a sample cell in the absence of the silica gel at temperatures from 294 to 345 K. Only the windows of the cell catalysed the reaction. The rate of the 9-bromoanthracene formation in this temperature range increased by a factor of 10. The surface coverage was kept constant throughout the temperature range by

Table 3

Temperature dependencies of the rise coefficients of the $9\text{-}C_{14}H_9Br$ at absence of silica gel

T^a (K)	$k'(9\text{-}C_{14}H_9Br)^b$ ($\times 10^{-4}$ s^{-1})
294.2	<0.1
307.9	0.70 ± 0.05
313.5	1.79 ± 0.04
315.4	1.56 ± 0.02
320.2	2.23 ± 0.02
325.9	2.33 ± 0.15
330.5	4.33 ± 0.05
331.9	4.13 ± 0.03
336.7	7.28 ± 0.05
336.9	7.65 ± 0.02
343.7	8.07 ± 0.03
344.1	10.3 ± 0.04
344.7	10.1 ± 0.03
345.0	8.60 ± 0.04

[a] Temperature uncertainty was ± 0.5 K.

[b] Temperature dependency of $k'(9\text{-}C_{14}H_9Br)$ is 50.33 ± 0.23 kJ mol^{-1}. The error limits are 1σ + Student's t and based on statistical uncertainties.

maintaining an excess amount of Br$_2$ in the solvent. In these conditions, a true activation energy E_a may be obtained by the Arrhenius expression. It was fitted to the rate coefficients k' measured at different temperatures to yield E_a to be 50.33 ± 0.23 kJ mol^{-1}. This value indicated the 9-

Fig. 3. UV fluorescence spectra of anthracene, 9-bromoanthracene, and 9,10-dibromoanthracene isolated in CCl$_4$. The resolutions of the spectra were 1.5 nm.

Table 4

Conditions and results of experiments used to measure the heat of the catalytic reaction $C_{14}H_{10} + Br_2 \rightarrow 9\text{-}C_{14}H_9Br + HBr$ and $9\text{-}C_{14}H_9Br + Br_2 \rightarrow 9{,}10\text{-}C_{14}H_8Br_2 + HBr$

$n_{C_{14}H_{10}}$ (mol)	n_{Br_2} (mol)	$\Delta_r H$ (kJ mol^{-1})	T (K)
1.756	1.846	−59.1	294.8
1.734	1.734	−55.7	293.6
1.779	1.833	−58.7	293.5
1.790	1.840	−59.9	292.6
1.767	1.783	−62.3	293.5

bromoanthracene formation on the catalyst as having strong temperature dependency and being chemical in nature. A vigorous constant agitation of the solution prevented the possibility of mass-transport limitation of the catalysed reaction. Because of the formation of the 9,10-dibromoanthracene, the uncertainty of the $k'(9\text{-}C_{14}H_9Br)$ increased in the temperature range from 343 to 345 K. At these temperatures, the possibility of a liquid phase bromination reaction was ruled out by adding IBr to a solution of Br$_2$/anthracene in CCl$_4$, forming no iodinated aromatic products (Table 4).

4. Discussion

4.1. Kinetics

As shown in Fig. 1, the rate of the 9-bromoanthracene formation per H atom is by a factor of 2.1 higher than that of the 9,10-dibromoanthracene, indicating Br as an electronegative substituent to diminish the rate of further bromination reaction. This conclusion is in accord with the results of another experiments, where 9-cyanoanthracene was not brominated at all in similar experimental conditions. By considering a mesomeric effect at the *para* position of an aromatic ring, the Br substituent has stronger ability to donate electrons to the ring than the cyano group has. It is actually an electron acceptor, which ability to attract electrons is large because of large electron affinity value [11]. Of the CN, Br, and H substituents, the cyano group has the largest and the H atom the smallest electron affinity value [12]. The operative electron transmission mechanism is conjugative in nature and stabilize the open shell structure via the Br substituent more than the CN substituent does after the *para*-C−H bond is ruptured.

The kinetics of the 9-bromoanthracene formation observed seemed to follow the first-order rate law, because the kinetic experiments were measured under first-order conditions, and the rate coefficient was linearly proportional to the catalyst weight. The kinetics measured resemble heterogeneous first-order wall reactions of the reactant in a tubular flow reactor [13].

For the beginning of the anthracene bromination reaction, the conditions were pseudo-first-order. The vacant silica gel sites were not rebrominated during the reaction. As the reaction proceeded, the Br atom concentration on silica gel surfaces as well as anthracene concentration in liquid
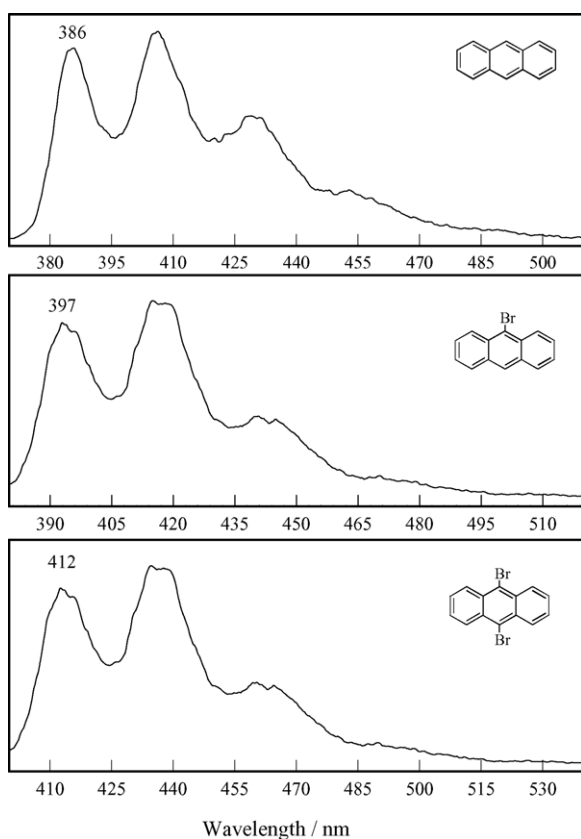
phase decreased. Results from the other experiments, however, have indicated the adsorption of anthracene on pure silica gel surfaces negligible. Furthermore, as Fig. 1 indicates, the 9-bromoanthracene molecules did not adsorb during the reaction on vacant adsorption sites of silica gel surfaces. The kinetics of the heterogeneous anthracene + $Br_2 \rightarrow$ 9-bromoanthracene + HBr reaction was monitored in situ either by use of the product formation signal or in similar conditions by the reactant decay signal. Both of these methods yielded very similar kinetic results, as shown by Table 1. It can thus be concluded that the side reactions may not be of an extent measurable by these kinetics.

Bromination of the 9-bromoanthracene occurred under pseudo-first-order conditions, because during the reaction the solvent contained a great excess of Br_2. This ensured that the silica gel used was constantly and completely saturated as the reaction proceeded by Br atoms, [Br]. A large Br_2 adsorption coefficient on the silica gel and high $[Br_2]$ in solution caused the equilibrium of the Br_2 adsorption to be clearly on the product side [14]. The adsorption with dissociation of Br_2 on silica gel seemed to follow the Langmuir adsorption isotherm, where the equilibrium was obtained in seconds under these experimental conditions. The $[Br_2]$ in liquid phase was large enough that the rate was zero-order in Br_2. This corresponds to the fully covered catalytic surface, so that the rate was determined by the amount of brominated surface sites. In these conditions, the rate law may still appear to be first-order in respect to the reactant 9-bromoanthracene: $v = k''[R]$, where k'' equals to $k \times b_R \times b_{Br}$ $[Br]^{-1}$. The absorbance signal profile of the 9,10-dibromoanthracene measured as a function of time was similar as the signal profile of the 9-bromoanthracene (see Fig. 1). This indicates that the 9,10-dibromoanthracene did not adsorb on the brominated silica gel surfaces. Moreover, compared with the catalytic bromination reactions, liquid phase bromination reactions had showed negligible rates. On the other hand, the rate of adsorption with dissociation of Br_2 on silica gel compared with the overall kinetics of the 9,10-dibromoanthracene formation, was very fast.

In the fluorescence kinetics of the 9-bromoanthracene, the precursore was brominated at similar conditions as the anthracene bromination. The silica gel was brominated before the 9-bromoantracene was added to the cuvette. The magnitudes of the rate coefficients obtained from absorption or fluorescence experiments were at similar conditions very close each other (see Table 2). This means that the closeness of the rate coefficients calculated from the signals of the reactant or the products indicates that there was only one parallel reaction present [15]. Thus, the anthracene or the 9-bromoanthracene did not have any side reactions at a measurable level.

Previously Altschuler and Berliner have studied a set of bromination reactions of aromatic hydrocarbons at various concentrations of acetic acid in water [2]. The reactions they measured were electrophilic substitution reactions with bromide ions present. The authors did not consider, however, the presence of catalytic bromination reactions on the walls of the reactor, which makes it difficult to compare their kinetic results to those of the current study.

4.2. Reaction mechanism

Bromination of the anthracene or the 9-bromoanthracene occurred at silica gel surfaces having only neutral or polarized species. Because of a large number of pores of molecular size, the surface area of silica gel is high. A large Bet surface area of the silica gel suggests that the smallest amount of silica gel used equals $33\,600\,cm^2$ of surface area compared with the window surface area value of $12\,cm^2$ of the sample cell. The windows of the cuvettes were quartz, which is SiO_2, thus resembling the hydrated silicon–oxygen compound built from SiO_4^{4-} tetrahedras. Both of these may be insulators, which can neither oxidized nor reduced. The ratio of the surface area values agrees with the ratio of the rate in these surface areas of bromination reactions (see Table 2). The bromination reactions are very slow (at 294 K) when the silica gel is absent. This is indicated in Fig. 1 by a small positive value of the intercept of the fitted straight line and the y-axis. The kinetics of the brominations reactions were not affected by the changes in bromine concentrations in solution, as also demonstrated previously [2].

Anthracene can be brominated completely to produce 9-bromoanthracene as the only aromatic product of the reaction. This product can in a similar manner be brominated completely to yield 9,10-dibromoanthracene. Another product in these reactions was indicated to be an acid by use of a litmus paper. This implies it to be HBr. The difference between the rates of brominations of the anthracene and the 9-bromoanthracene makes it possible to isolate the native 9-bromoanthracene molecules from the solution. In general, the bromination reaction, which are substitution reactions, requires Br_2 to have a dissociative adsorption on clean silica gel surfaces. The Br_2 may initially be attracted on the surface by an electron transport from the solid to the molecule making it polarized. This is followed by an adsorption reaction of anthracene on the brominated silica gel. After this, the heterogeneous reaction proceeds by replacing the H at the 9 position by a Br atom. HBr may be formed by another Br-atom abstracting an H-atom from the precursore. This mechanism was explored by the following set of experiments: (1) the silica gel was completely covered by Br atoms, (2) the remaining Br_2-containing CCl_4 in the cell was replaced by 2.0 ml of IBr-containing CCl_4, and (3) 1.0 ml of the $C_{14}H_{10}$-containing CCl_4 liquid was added to the cell under constant mixing. No indications of iodinated anthracene were detectable in the reaction cell. This result indicates that the H-atom substitution reaction occurs only at silica gel surfaces, not in the liquid phase. The liquid phase did not contain 9-anthryl free radicals. On the other hand, if IBr dissociatively adsorbs on the silica gel surface, it may brominate anthracene, but not iodinate it. This is because the energy barrier of the H-atom abstraction reaction by an I atom is typically twice as large as that of a Br atom reaction. The Br atom is more

reactive than the I atom. Both the bromination reactions of the current study reveal that the C–H bonds at the 9 and 10 positions of the anthracene and at the 10 position of the 9-bromoanthracene were weaker than the other C–H bonds of these molecules.

4.3. Heat of the reaction

In the calorimetric measurements the bromination reaction was catalyzed by the glass walls of the Dewar flask. The surface area (about $180\,cm^2$) of the walls was large enough to complete the anthracene bromination reaction in 200 s. The number of moles of Br_2 and the anthracene were equal.[2] At these conditions only 9-bromoanthracene was formed. This was ensured by comparing ^1H NMR spectra of the reaction product to those of the 9-bromoanthacene and of the 9,10-dibromoanthracene.

In another set of experiments the 9-bromoanthracene as a reactant was brominated quite slowly to give the 9,10-dibromoanthracene as a product. The reaction is so slow that the exothermic adsorption of Br_2 on the walls of the reactor disturbed the data collection. However, it can be concluded that the formation of the 9,10-dibromoanthracene is clearly exothermic reaction.

4.4. Spectroscopic information

All of the compounds studied are classified into the acenes. Their absorption spectra are similar. In the case of the anthracene, the strong absorption may belong to the main series of $^1B_b \leftarrow {}^1A$ transition (highly allowed), and the weaker absorptions may belong to the secondary series of $^1L_a \leftarrow {}^1A$ [16]. The latter is partially forbidden transition thus having a low intensity. A similar designation may be used for the 9-bromoanthracene and the 9,10-dibromoanthracene. After anthracene is brominated at the 9, and at the 9 and 10 positions, the ^1L_a band series is red-shifted. The vertical $0 \leftarrow 0$ transition is red-shifted, similarly.

The emission spectra of acenes measured have a structure of 4 wide emission peaks (see Fig. 3), which for cata-condensed polyaromatic conjugated compounds is quite common [17]. The average spacing of the $^1L_a \leftarrow {}^1A$ absorptions among the compounds measured is $1427 \pm 20\,cm^{-1}$. A similar comparisons of the fluorescence signals gives about

$100\,cm^{-1}$ smaller value because of the vibrational deactivation at the excited state of the molecule.

5. Summary

The heterogeneous kinetics of the catalytic bromination of anthracene and 9-bromoanthracene on silica gel have been characterized. The rate per H-atom of the 9-bromoanthracene formation from the anthracene is by a factor of 2.1 higher than the 9,10-dibromoanthracene formation from the 9-bromoanthracene. Arrhenius activation energy and the heat of the reaction of the 9-bromoanthracene formation were 50.3 and $-59.1\,kJ\,mol^{-1}$.

Acknowledgements

References

[1] K. Lauer, R. Oda, Ber. Dtsch. Chem. Ges. 69B (1936) 978.
[2] L. Altschuler, E. Berliner, J. Am. Chem. Soc. 88 (1966) 5837.
[3] H.A. Muathen, J. Org. Chem. 57 (1992) 2740.
[4] S. Dwan, J. Turk, J. Speigle, J. Corbin, J. Masnovi, R.J. Baker, J. Org. Chem. 65 (2000) 3005.
[5] O.L. Wright, L.E. Mura, J. Chem. Educ. 43 (1966) 150.
[6] M. Ghiaci, J. Asghari, Bull. Chem. Soc. Jpn. 74 (2001) 1151.
[7] E. Clar, Spectrochim. Acta 4 (1950) 116.
[8] http://www.nist.gov.
[9] F. Wilkinson, Chemical Kinetics and Reaction Mechanism, van Nostrand Reinhold, 1980, p. 231.
[10] J.W. Williams, F. Daniels, J. Am. Chem. Soc. 46 (1924) 1569.
[11] J.N. Murrell, The Theory of the Electronic Spectra of Organic Molecules, Wiley, New York, 1963.
[12] S.G. Lias, J.E. Bartmess, J.F. Liebman, J.L. Holmes, R.D. Levin, W.G. Mallard, J. Phys. Chem. Ref. Data 17 (Suppl. 1) (1988).
[13] J.A. Seetula, J. Chem. Soc., Faraday Trans. 92 (1996) 3069.
[14] M.J. Rosen, J. Gandler, J. Phys. Chem. 75 (1971) 887.
[15] J.I. Steinfeld, J.S. Francisco, W.L. Hase, Chemical Kinetics Dynamics, 2nd ed., Prentice-Hall, 1998.
[16] V.H. Zimmermann, N. Joop, Ber. Bunsen-Ges. Phys. Chem. 66 (1962) 342.
[17] T. Nagamura, T. Nakayama, K. Hamanoue, Chem. Lett. 20 (1991) 2051.